Torque Ripple Analysis of Speed Control Techniques of BLDC Motor for EV Applications

Amit B. Jadhav [1], Dr. Mahadev S. Patil [2]

[1] Department of Electrical Engineering, D. Y. Patil Education Society (Deemed to be University) School of Engineering & Management, Kolhapur, Maharashtra-416006, India and Research Scholar, Shivaji University, Kolhapur Maharashtra-416006, India

[2] Department of Electronics & Telecommunication Engineering, Kasegaon Education Society's Rajarambapu Institute of Technology, Affiliated to Shivaji University , Sakharale, Maharashtra-415414, India

[1]amitbhimraojadhav@gmail.com, [2]mahadev.patil@ritindia.edu

Abstract

In BLDC motor operation torque ripples affects performance, efficiency and application suitability. The torque ripples are cyclical variations in output torque during motor rotation, creating undesirable consequences including increased noise, vibrations, reduced efficiency and compromised precision in positioning applications. Torque ripples are characterized as the variance of output torque as the motor rotates, representing a deviation from the idealized constant torque output. Torque ripples are caused due to non-ideal current waveform due to commutation action are undesirable for smooth motor operation and will cause oscillations in the speed of the motor. These oscillations increase the noise and vibrations of the mechanical parts of the motor thus reducing the lifespan of the motor. The torque ripples fundamentally impact the motor's ability to deliver smooth, consistent power transmission. In this paper, torque ripple analysis of BLDC motor is presented using MATLAB simulations with FOC control, SMC control and PWM control techniques. The current ripple minimization is the primarily focused which also reduces the torque ripples in the BLDC motor for wide range of operating speed. The FOC control outperforms for reducing torque ripples with 10% ripples in motor output torque.

Keywords: BLDC motor, speed control, torque ripples, FOC, PWM

1. Introduction

BLDC motors are favoured for EVs due to their superior efficiency, durability and performance characteristics. Unlike traditional brushed motors, BLDC motors eliminate physical brushes and commutators, instead utilizing sophisticated electronic controllers to precisely switch

current through stationary stator windings. This creates a rotating magnetic field that drives a permanent magnet rotor [1]. The absence of brushes significantly reduces maintenance needs and enhances long-term reliability. BLDC motors achieve 85–90% efficiency, significantly reducing energy loss compared to brushed motors. This efficiency translates to longer driving range. BLDC motors deliver high torque density in compact designs, enabling lighter vehicles without sacrificing acceleration or performance [2]. The electronic commutation allows real-time adjustments to speed and torque, enhancing driving dynamics and responsiveness [3]. The permanent magnets in BLDC motor makes it to work as generator and hence integrate the regenerative braking in EV. The regenerative braking can recharge the EV battery and hence contributes for increasing travel range per charging of battery [4]. The permanent magnet motors are characterized by their high power density, superior efficiency across a broad operating range, and excellent torque capability, making them highly desirable for maximizing vehicle range and performance. On the other hand SRM and induction motors are preferred for development of cost effective EVs and particularly suitable for inherent robustness and fault tolerance [5].

The precise and dynamic speed control is paramount for electric vehicles. The most fundamental and widely used method for regulating BLDC motor speed is Pulse Width Modulation (PWM) control of the applied voltage [6]. The PWM controller adjusts the *average* voltage supplied to the motor windings by varying the duty cycle of the PWM signal – the ratio of "on" time to the total switching period. A higher duty cycle means the transistors are on for a larger portion of the time, delivering a higher average voltage to the windings. This increased voltage results in higher current flow, strengthening the stator's magnetic field. Consequently, the motor develops more torque to overcome its load and inertial forces, accelerating it to a higher rotational speed. Conversely, reducing the PWM duty cycle lowers the average voltage and current, weakening the magnetic field and thus reducing the motor's torque and speed [7]. This method provides smooth and efficient speed regulation across a wide operating range, directly linking the commanded speed to the electrical power input [8]. The discontinuous nature of PWM current pulses also leads to current ripple, causing undesirable torque pulsations (ripple) and potential mechanical vibrations, even at steady-state speeds, impacting smoothness. Additionally, the effective voltage applied is inherently lower than the DC bus voltage due to the PWM process, limiting the maximum achievable torque at very low speeds [9, 10].

For minimizing the current ripples and thereby the torque ripples, current controllers are deployed in BLDC control. The hysteresis control technique for speed control, the measured phase current is compared to a sinusoidal reference current. If the actual current exceeds the reference plus a hysteresis band, the corresponding inverter leg switches to decrease the current. Conversely, if it falls below the reference minus the band, the leg switches to increase the current. This forces the actual current to track the reference within the defined hysteresis band. Its main advantages are simplicity, very fast dynamic response, inherent current limiting, and lack of a fixed switching frequency. However, it leads to variable switching frequency (causing EMI issues), potentially high switching losses, and phase current distortion, especially at higher speeds or with small hysteresis bands [11, 12].

The Sliding Mode Control (SMC) technique is well-suited for systems with uncertainties and disturbances, like motor drives [13]. It defines a sliding surface a function of the speed error and its derivative. The control law is designed to drive the system state onto this surface and then keep it sliding along the surface towards the desired zero error point by applying discontinuous control actions of inverter states. SMC is highly robust against parameter variations, load torque disturbances and modelling inaccuracies. It offers fast dynamic response. However, the inherent discontinuous control action causes high-frequency chattering, potentially damaging switching of the inverter states. The minimization of this chattering is achievable through adaptive SMC and adding boundary layers at the cost of increased complexity [14].

Field-Oriented Control (FOC) is a sophisticated technique for speed control of BLDC motor to achieve the performance similar to that of separately excited DC motor, where torque and flux can be independently controlled [15]. It is based on mathematically transforming the measured three-phase stator currents into a two-axis rotating reference frame synchronized with the rotor's magnetic flux position [16]. In this transformed frame, the direct-axis current (I_d) primarily controls the motor's magnetic flux, while the quadrature-axis current (I_q) governs electromagnetic torque production. Independent PI controllers regulate I_d and I_q to match their reference values. The output voltage commands from these PI controllers are then transformed back into the three-phase stationary reference frame using inverse transformations, generating the PWM signals for the inverter. The key advantage of FOC is this decoupling, enabling exceptionally smooth torque output with minimal ripple, high efficiency across a wide operating range, precise dynamic response and optimal torque per ampere [17]. The FOC demands accurate and continuous rotor position feedback, significant computational power for

the real-time coordinate transformations (Clarke/Park and inverse), tuning of multiple PI controllers, and is sensitive to motor parameter variations (like resistance and inductance), making its implementation more complex and costly than simpler trapezoidal control methods. Despite these challenges, FOC's superior performance in torque smoothness and efficiency makes it the dominant control strategy for high-performance EV motors [18].

While standard BLDC control often relies on Hall effect sensors for rotor position feedback, these sensors introduce drawbacks including cost, reduced reliability in harsh environments, susceptibility to electromagnetic interference (EMI), and additional assembly complexity. The sensor less control [19] eliminates the requirements of hall sensors for the control schemes and reduces the amplitude of the inverter current, reduces the noise emitted by the running motor and the EMC interference emitted to the environment. Various direct torque control techniques for precise control of torque are discussed in [20].

The BLDC motors inherently suffer from torque pulsations that create operational challenges. The torque ripple in these motors produces detrimental effects including increased noise, vibrations and reduced efficiency [21]. Torque ripple in BLDC motors arises from several inherent design and operational factors, degrading smooth operation and causing vibration and acoustic noise. The most significant source is commutation torque ripple, inherent to the standard trapezoidal control strategy. During each 60-degree electrical commutation interval, only two phases are actively conducting while the third is switched off. The rapid transfer of current between phases at commutation instants causes discontinuous current waveforms, leading to pulsations in the instantaneous torque produced. This is exacerbated by imperfect current build-up and decay due to winding inductance, especially at higher speeds. The non-ideal back-EMF waveform contributes substantially. While ideal trapezoidal control assumes perfectly trapezoidal phase back-EMF waveforms with 120-degree flat tops, real motor designs often produce back-EMF that is more sinusoidal or has significant harmonics due to stator slotting, magnet shape or magnetic saturation. This mismatch between the assumed ideal waveform and the actual voltage induced in the windings prevents perfect alignment of current and back-EMF, reducing average torque and increasing ripple [22]. The cogging torque is caused by the interaction between the permanent magnets on the rotor and the slotted stator structure, produces periodic torque pulsations even when the motor is unpowered. This reluctance torque is most pronounced at low speeds and during startup, creating a "cogging" effect. PWM-induced current ripple, delays in current controllers and

sensor inaccuracies prevent the ideal current waveforms from being achieved and hence causing torque ripples [23].

In this paper torque ripple and dynamic performance analysis of PWM, SMC and FOC speed control techniques for BLDC motor is presented with MATLAB simulation. This analysis is useful for selecting appropriate speed control technique for BLDC motor in EV applications.

2. Speed Control Techniques

A. PWM Speed Control

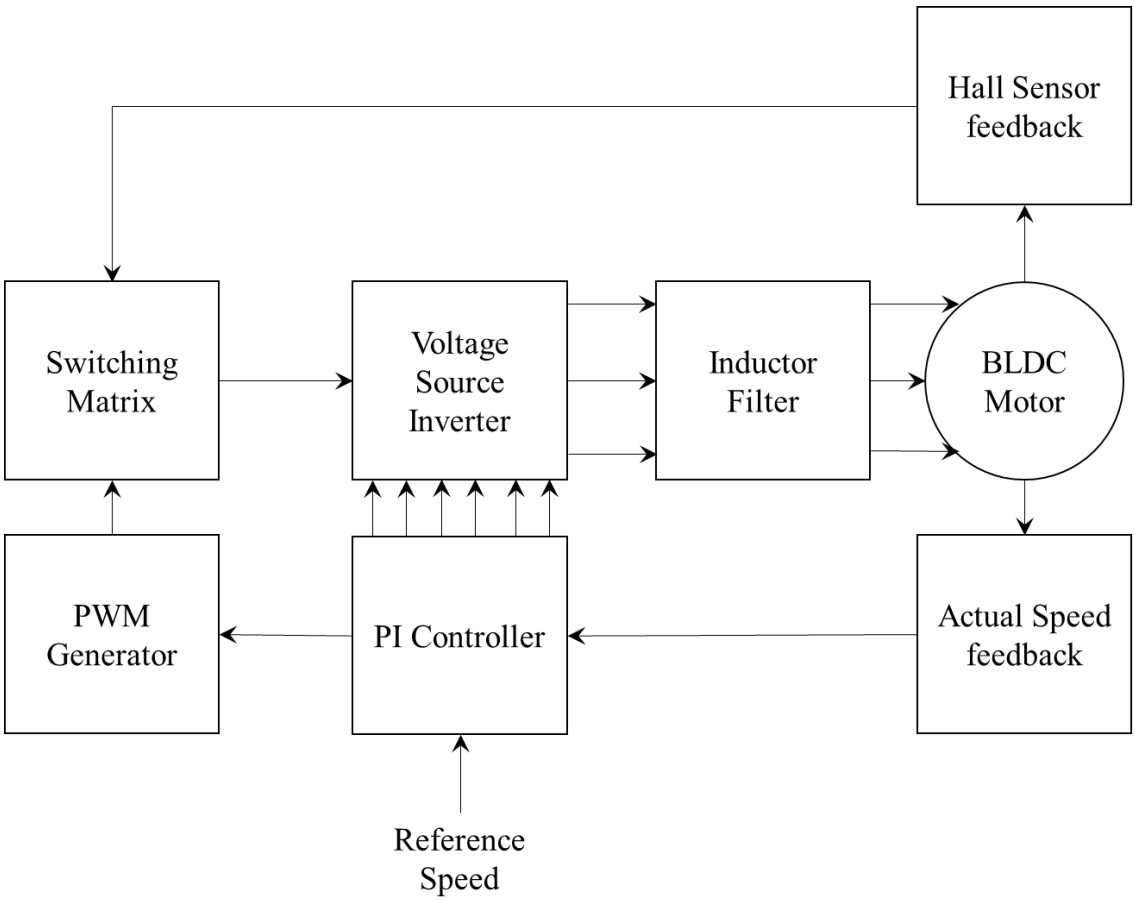

Figure 1: PWM Speed control of BLDC motor

Figure 1 shows PWM speed control system for BLDC motor. The difference between desired speed and actual speed is fed as input to a PI Controller. The PI Controller generates a corrective signal based on any speed error. This signal is sent to a PWM generator, which produces the PWM pulses with a variable duty cycle. The switching matrix uses the Hall Sensor feedback to determine the precise rotor position and electronically commutate the motor. It routes the PWM signals to the appropriate switches of the inverter. The inverter

converts DC power into three-phase AC with variable voltage and frequency, applying it to the BLDC Motor to drive it. The Hall Sensors continuously provide rotor position data, enables the correct commutation sequence with switching matrix and the calculation of the actual speed for feedback to the PI Controller. This continuous loop allows the system to maintain the motor speed at the desired reference value, automatically compensating for load changes or disturbances.

B. SMC Control

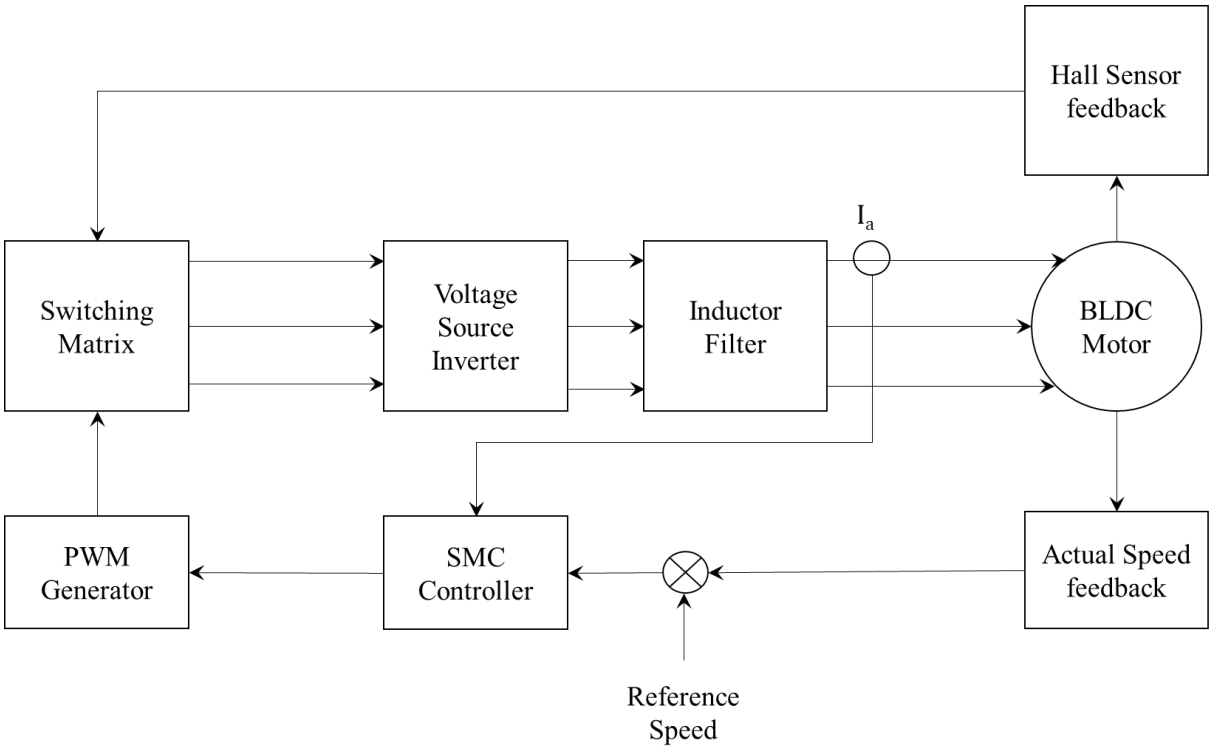

Figure 2: Control Scheme for SMC Control of BLDC motor

The sliding mode control (SMC) of a BLDC motor is shown in figure 2. The process of SMC starts with the reference speed, which serves as the desired speed input for the motor. The difference between reference speed and actual speed is calculated as the speed error. The SMC speed controller processes this error using sliding mode control laws. The SMC controller generates a reference current, which is compared with the measured phase currents from the BLDC motor. The SMC current controller uses these current errors to produce highly responsive and accurate control actions, generating the switching signals needed for the voltage source inverter. The inverter, guided by these switching commands, supplies the regulated voltage and current to the BLDC motor to ensure it follows the desired speed profile. The speed

and rotor position feedback obtained using hall sensors, are continuously provided to the control system, allowing the SMC scheme to quickly react to disturbances or changes in operating conditions. This dual-loop SMC approach, with speed and current loops, offers superior dynamic response, fast current regulation and excellent resilience to parameter variations, making it ideal for demanding BLDC motor applications.

C. FOC Control

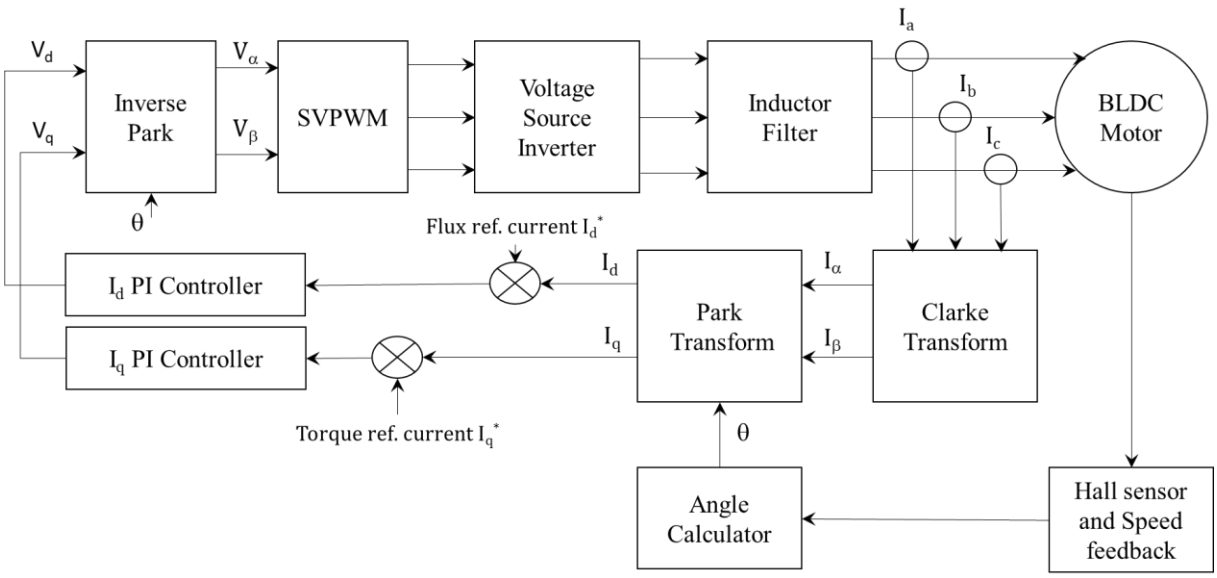

Figure 3: Control Scheme for FOC Control of BLDC motor

The figure 3 illustrates FOC control structure for precise BLDC motor speed regulation. The outer speed control loop starts with a reference speed compared against the actual motor speed from a position/speed sensor. The resulting speed error drives a PI speed controller, which outputs a torque reference, typically represented as the quadrature-axis current reference (I_q*). The direct-axis current reference (I_d*) is set to zero for maximum torque per ampereoperation. These dq-axis current references enter the fast inner current control loop, where they are compared against actual dq currents (I_d, I_q). The actual currents are derived by measuring motor phase currents (I_a, I_b, I_c), transforming them to the stationary αβ-frame using the Clarke transform, then to the rotating dq-frame aligned with the rotor flux using the Park transform (requiring rotor angle θ from the sensor). PI current controllers process the d/q-axis current errors and generate dq-axis voltage commands (V_d, V_q). The Inverse Park transform converts these rotating-frame voltages back to the stationary αβ-frame (V_α, V_β) using θ. Space Vector Modulation then translates these αβ voltages into PWM signals for a 3-phase inverter, which drives the BLDC motor windings with sinusoidal currents. By continuously

transforming currents into the rotor's rotating frame, FOC decouples torque (I_q) and flux (I_d) control, enabling smooth, efficient and dynamic motor performance similar to a DC motor, while the nested loops ensure accurate speed tracking and disturbance rejection.

3. Simulation and Results

The MATLAB Simulink model is built for speed control of BLDC motor with three control techniques namely- PWM Control, SMC control and FOC control. The simulation results are analysed for speed tracking, response to reference speed change, torque ripples and dynamic speed characteristics. The system specifications are mentioned in table 1. The same specifications are used for all the speed control techniques.

Table 1: System Specifications

Parameter	Details
DC Source	Battery – 48V, 20Ah
BLDC Motor Characteristics	Inductance = 8.5mH Resistance = 0.05Ω Poles = 4 Rated Torque = 2 NM
Inverter	Three phase full bridge
Feedback	Hall sensor
Switching frequency	10kHz
Filter	Inductor – 2.6mH

A. PWM Control

The BLDC motor speed control system with PWM control is simulated for various speed steps for a period of 5 seconds. The torque input to the BLDC motor is set at 2 NM. The speed response against the reference speed is seen in figure 4. In the graph of the actual speed, oscillation are observed when the reference speed is changed. To achieve a steady speed after change in reference speed, as seen in figure 5, the system take 0.21 second to settle when reference speed is changed from 200 RPM to 500 RPM. The system takes 0.07 seconds for

every 100RPM speed change. The steady state error (difference between reference and actual speed) is recorded to be 0.3%.

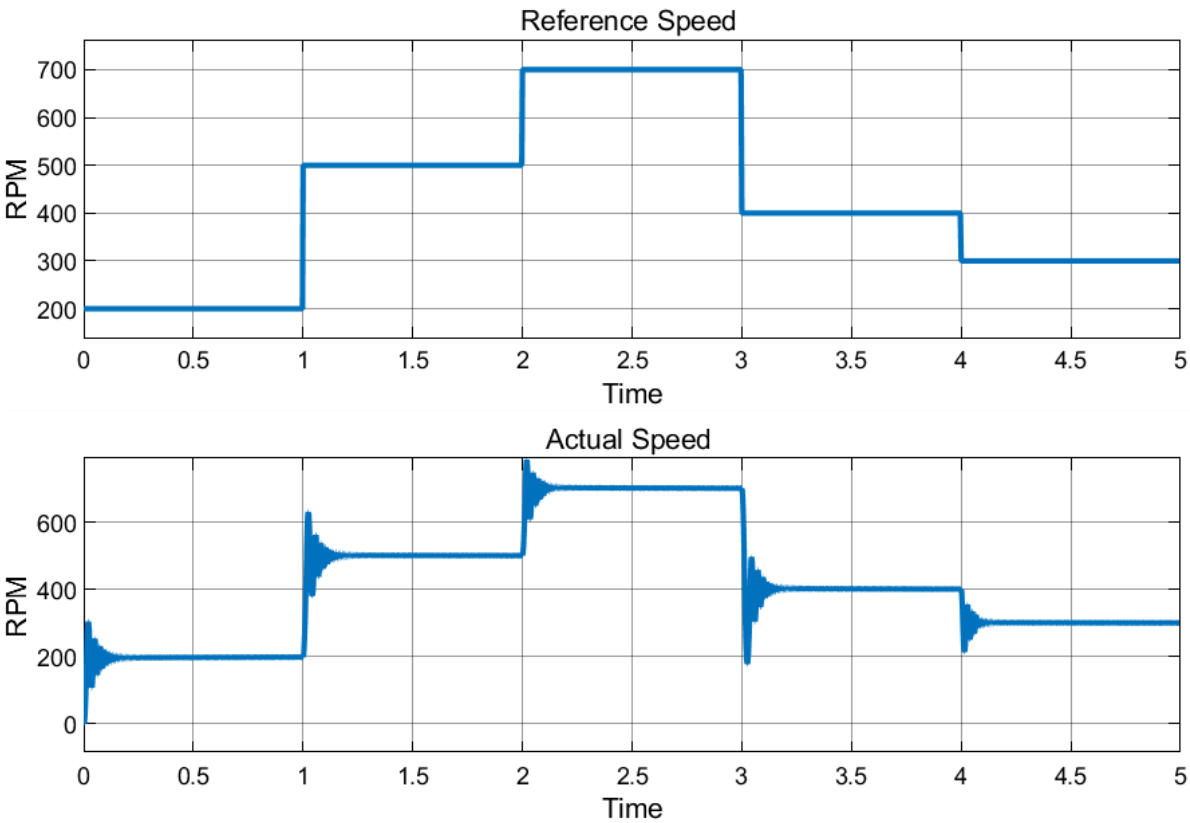

Figure 4: Reference Speed and actual speed.

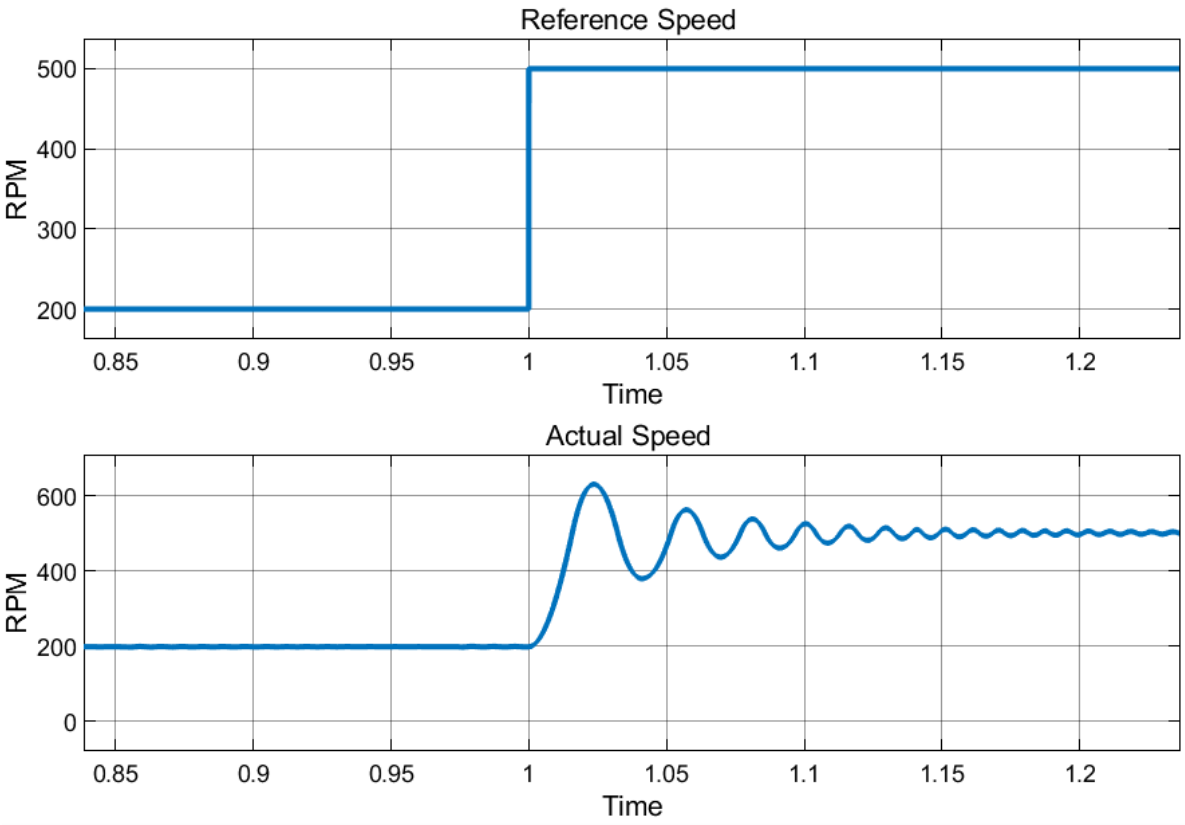

Figure 5: Zoomed view of speed Response for step change from 200RPM to 500 RPM

The torque response of the speed control system over the operating speed range is shown in figure 6. The torque input (load) to the motor is set at 2 NM. When reference speed is changed, a large the torque pulsation is observed. This pulsation settles as the actual speed approaches the reference speed. In the graph of the torque response the motor output torque is seen to be fluctuating around reference value in steady state. A zoomed view of this torque response during motor speed of 500 RPM is recorded as seen in figure 7. The torque ripples are calculated by noting their peak to peak value in oscillating state. The torque ripples are observed to be 100%.

$$\tau_{pp} = 2.0$$

$$\tau_{ref} = 2.0$$

$$\tau_{ripple} = \frac{\tau_{pp}}{\tau_{ref}} \times 100 = \frac{2}{2} \times 100 = 100\%$$

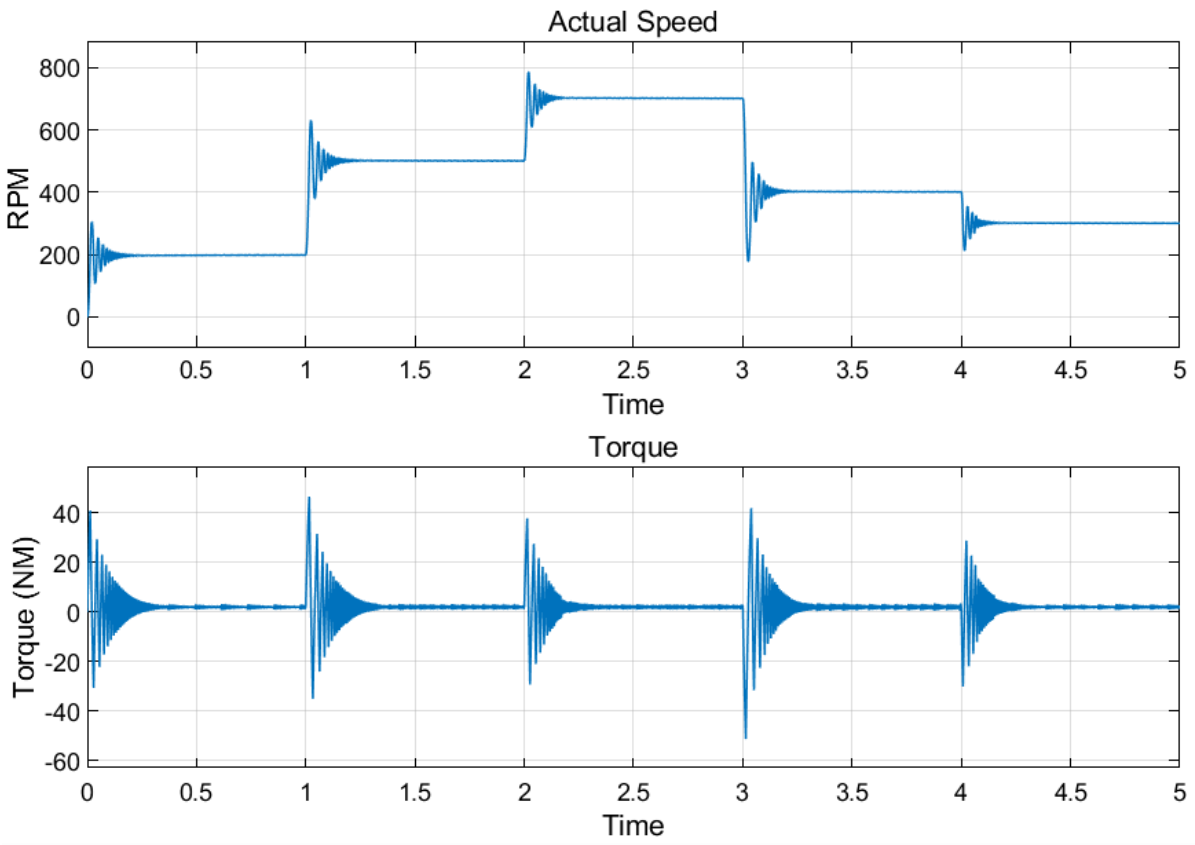

Figure 6: Torque response

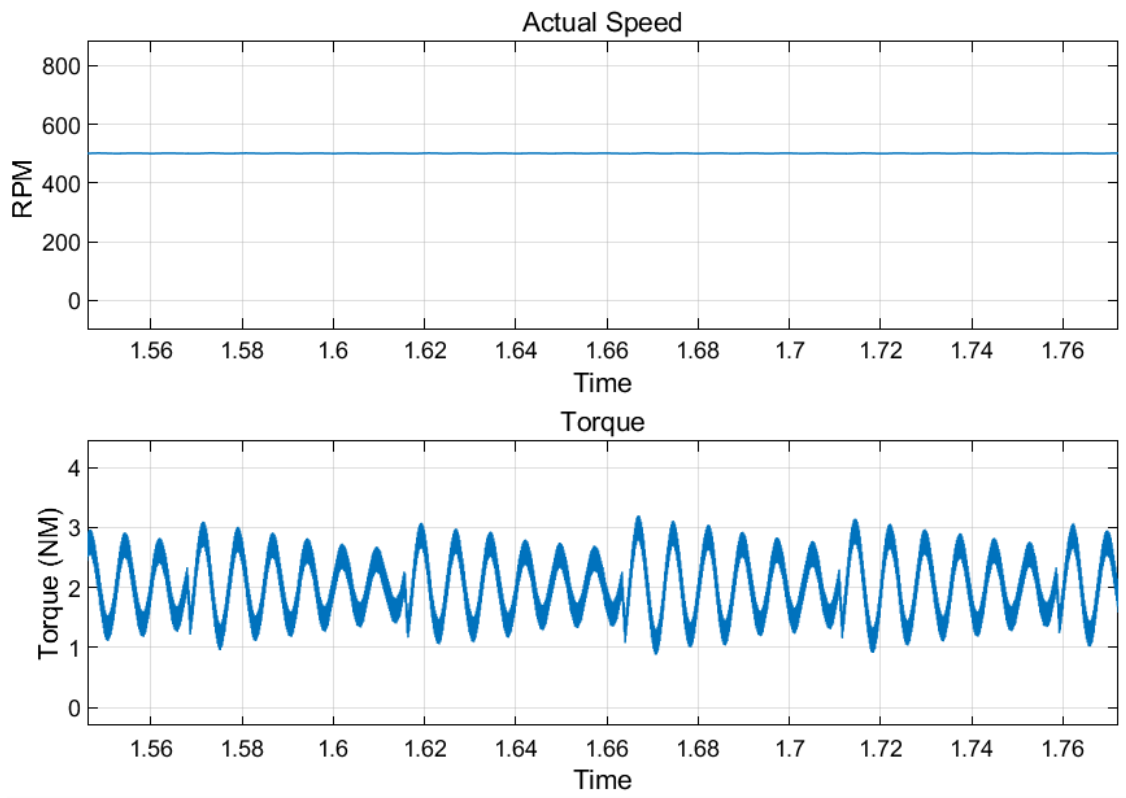

Figure 7: Zoomed view of torque response at 500 RPM speed

B. SMC Control

The system of SMC based BLDC motor control is simulated for various speed steps for a period of 5 seconds. The torque input to the BLDC motor is set at 2 NM. The speed response against the reference speed is seen in figure 8. In the graph of the actual speed, oscillation are observed when the reference speed is changed. To achieve a steady speed after change in reference speed, as seen in figure 9, the system take 0.3 second to settle when reference speed is changed from 200 RPM to 500 RPM. The system takes 0.1 seconds for every 100RPM speed change. The steady state error (difference between reference and actual speed) is recorded to be 0.5%.

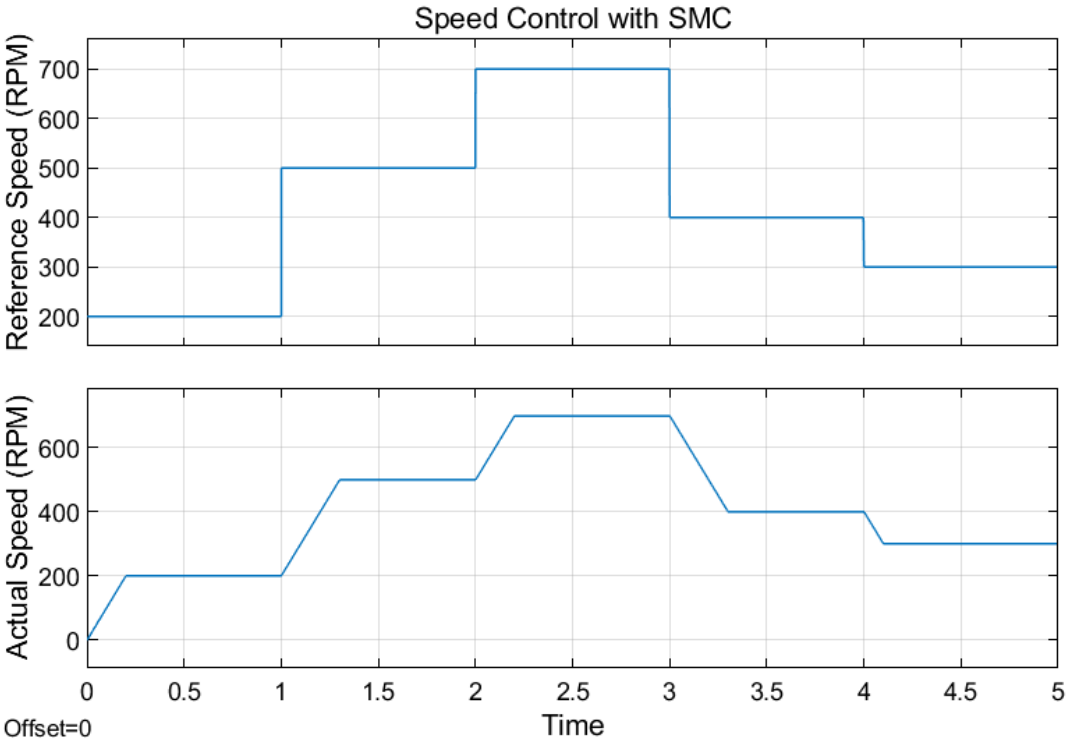

Figure 8: Reference Speed and actual speed.

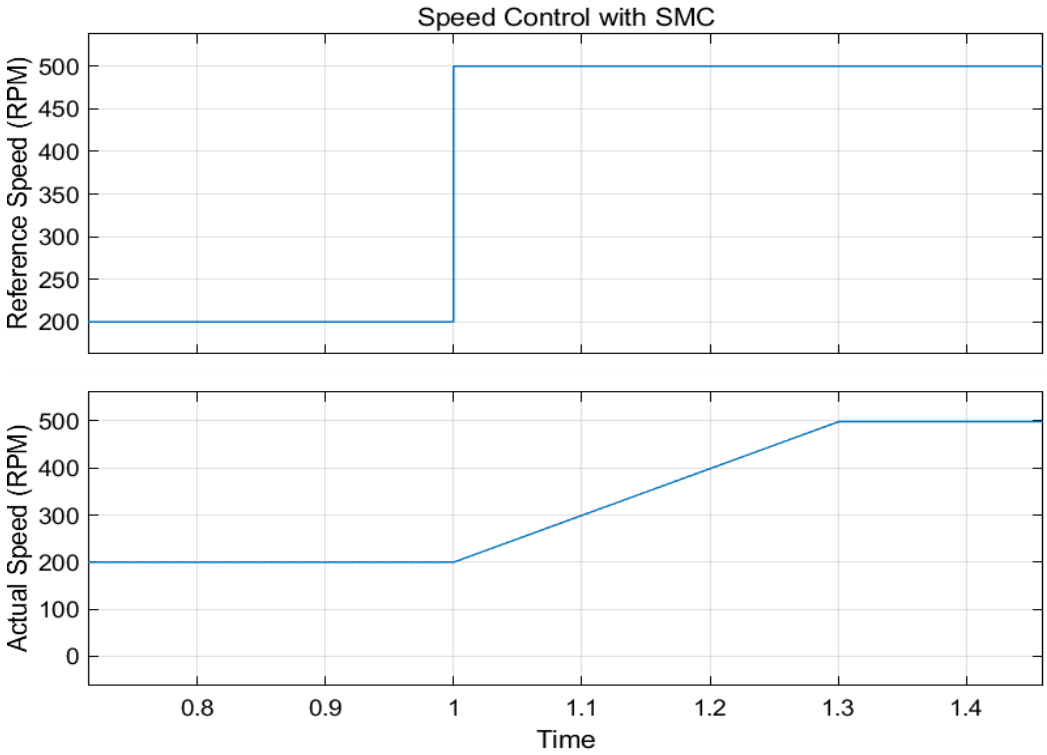

Figure 9: Zoomed view of speed Response for step change from 200RPM to 500 RPM

The torque response of the speed control system over the operating speed range is shown in figure 10. The torque input (load) to the motor is set at 2 NM. When the motor start from zero speed, large torque ripples are seen. As the actual speed approaches the reference speed, torque ripples are gradually reduced. When reference speed is changed, a torque change is observed in the direction of new reference speed. This torque change settles to the reference value as the actual speed approaches the reference speed. In the graph of the torque response the motor output torque is seen to be fluctuating around reference value in steady state. A zoomed view of this torque response during motor speed of 500 RPM is recorded as seen in figure 11. The torque ripples are calculated by noting their peak to peak value in oscillating state. The torque ripples are observed to be 100%.

$$\tau_{pp} = 0.4$$

$$\tau_{ref} = 2.0$$

$$\tau_{ripple} = \frac{\tau_{pp}}{\tau_{ref}} \times 100 = \frac{0.4}{2} \times 100 = 20\%$$

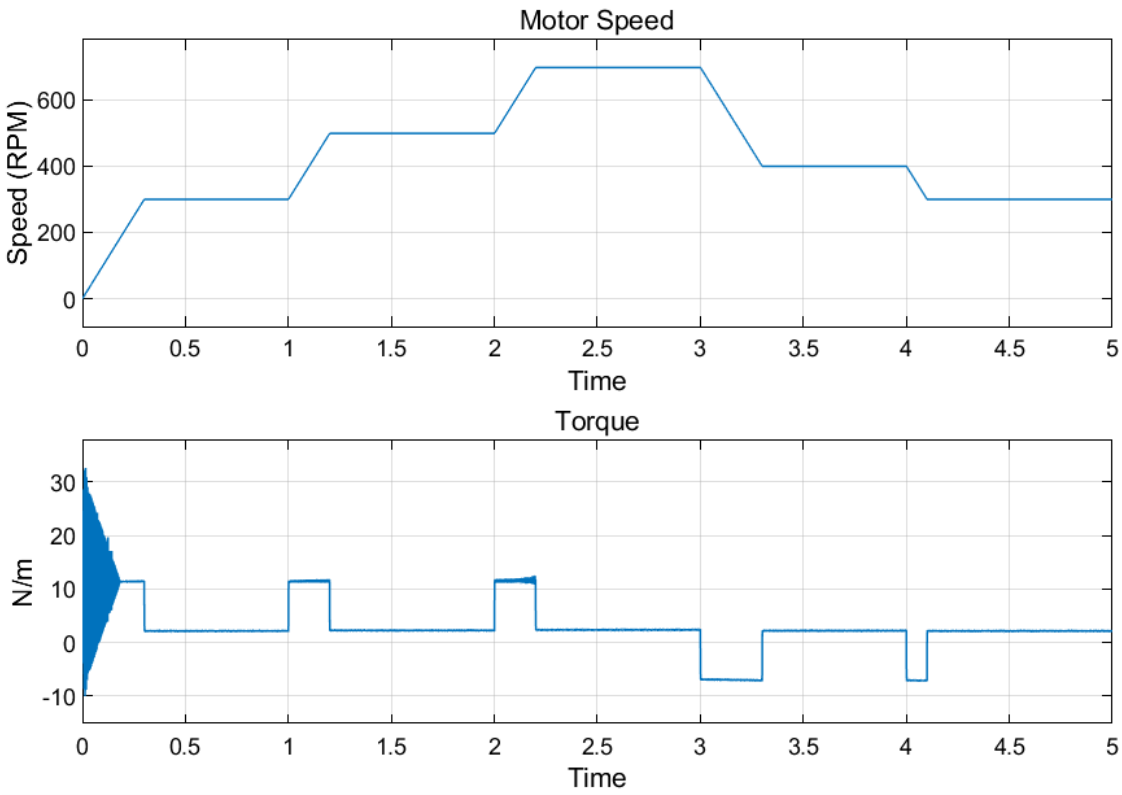

Figure 10: Torque response

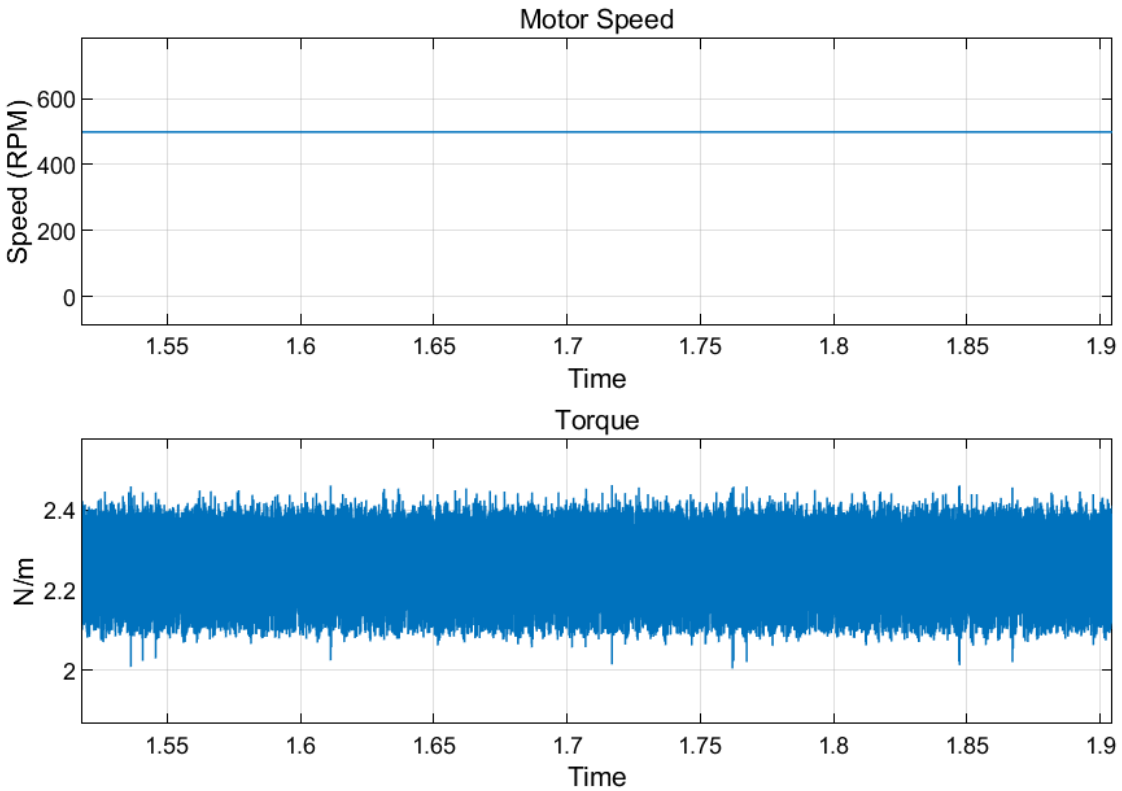

Figure 11: Zoomed view of torque response at 500 RPM speed

C. FOC Control

The system is simulated for various speed steps for a period of 5 seconds. The torque input to the BLDC motor is set at 2 NM. The speed response against the reference speed is seen in figure 12. In the graph of the actual speed, oscillation are observed when the reference speed is changed. To achieve a steady speed after change in reference speed, as seen in figure 13, the system take 0.05 second to settle when reference speed is changed from 200 RPM to 500 RPM. The system takes 0.016 seconds for every 100RPM speed change. The steady state error (difference between reference and actual speed) is recorded to be 1%.

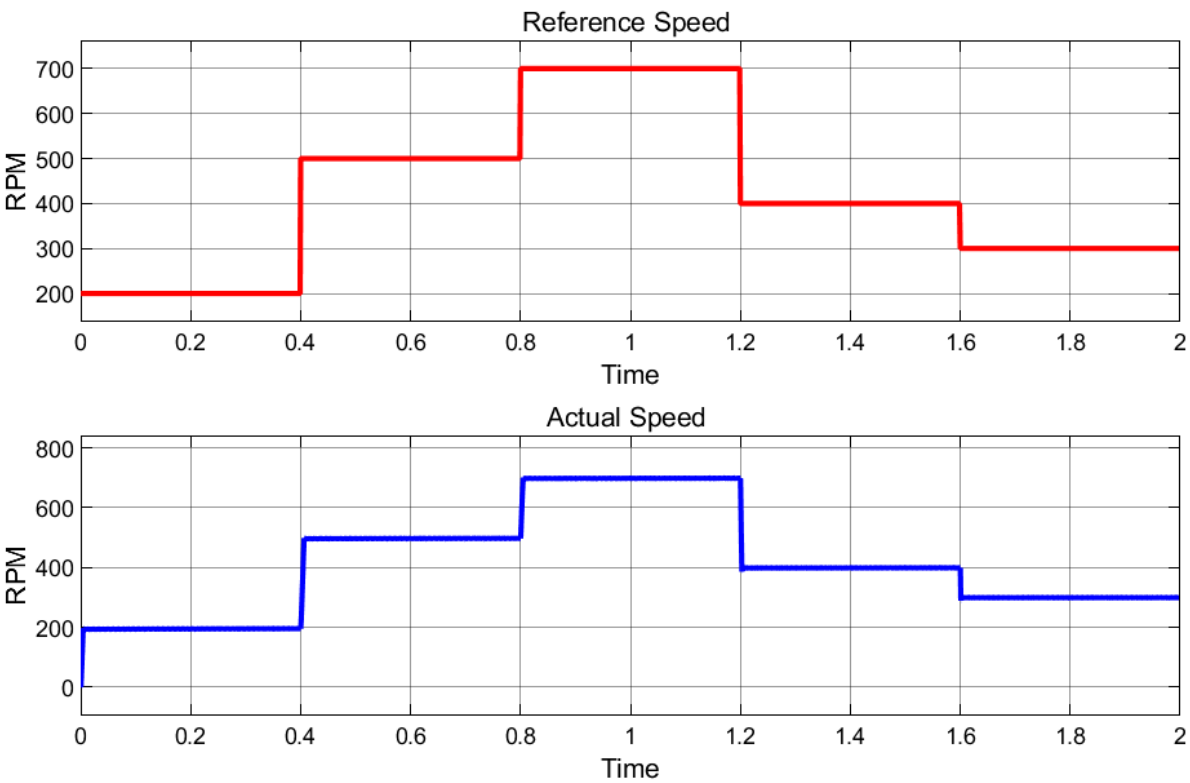

Figure 12: Reference Speed and actual speed

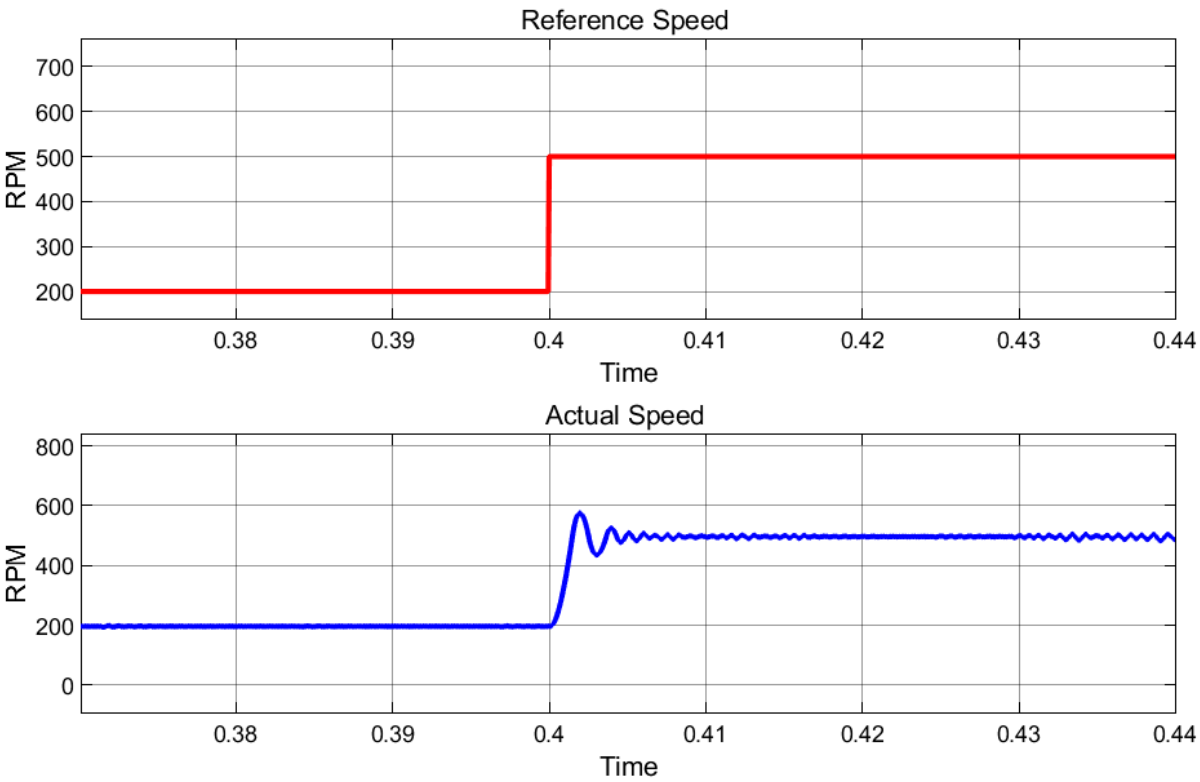

Figure 13: Zoomed view of speed Response for step change from 200RPM to 500 RPM

The torque response of the speed control system over the operating speed range is shown in figure 14. The torque input (load) to the motor is set at 2 NM. When reference speed is changed, a large the torque change is observed in the direction of speed change. The actual torque value settles to reference value as the actual speed approaches the reference speed. In the graph of the torque response the motor output torque is seen to be fluctuating around reference value in steady state. A zoomed view of this torque response during motor speed of 500 RPM is recorded as seen in figure 15. The torque ripples are calculated by noting their peak to peak value in oscillating state. The torque ripples are observed to be 10%.

$$\tau_{pp} = 0.2$$

$$\tau_{ref} = 2.0$$

$$\tau_{ripple} = \frac{\tau_{pp}}{\tau_{ref}} \times 100 = \frac{0.2}{2} \times 100 = 10\%$$

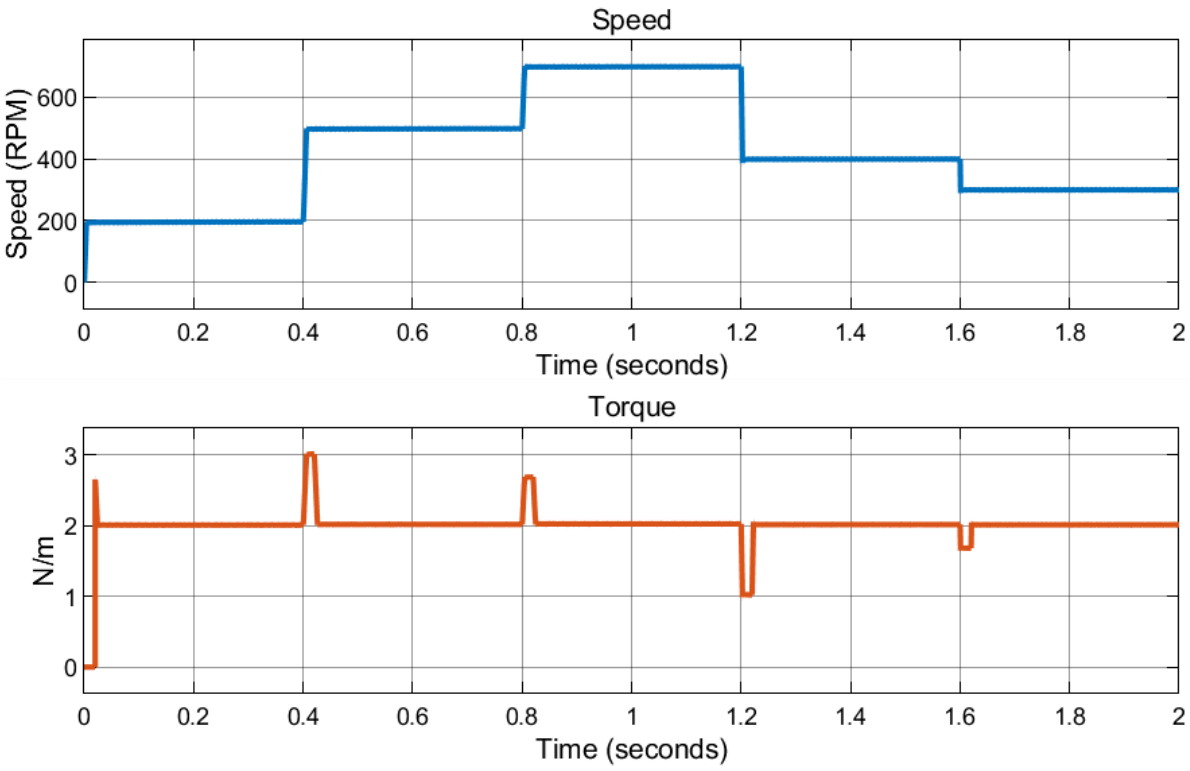

Figure 14: Torque response

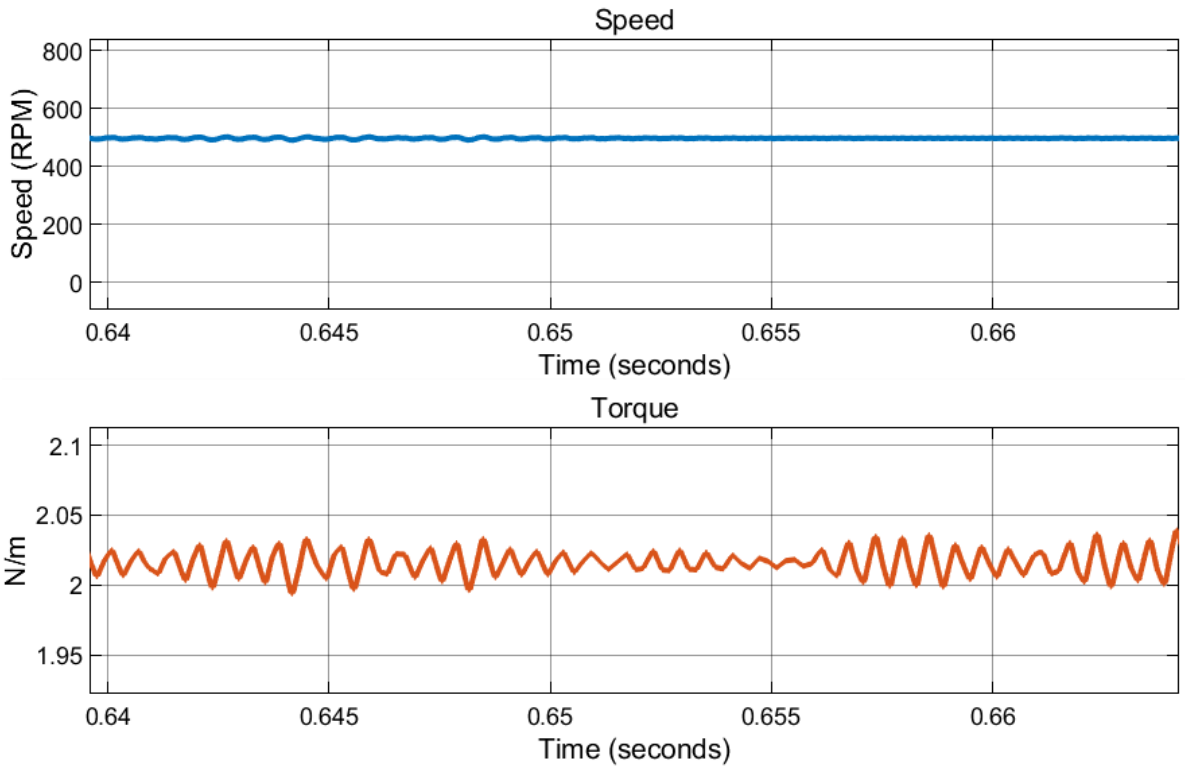

Figure 15: Zoomed view of torque response at 500 RPM speed

Table 2: Comparative of dynamic performance

Technique	Steady State Error (%)	Settling Time (S/ 100RPM)	Torque Ripple (%)
PWM Control	0.3	0.07	100%
SMC Control	0.5	0.1	20%
FOC Control	1	0.05	10%

The comparison of speed control techniques at steady state and transient state is illustrated in table 2. Steady-State Error measures how accurately the motor maintains its target speed once stable (lower % is better). Settling Time indicates how quickly the motor reaches and stabilizes at a new target speed after a command is given to change the reference speed (lower seconds per 100 RPM is better). The steady state error with PWM technique is least among the control techniques compared, however, in terms of the settling time i.e. dynamic response, FOC outperforms PWM control and SMC control. From figure 9, the SMC control shows no overshoots or undershoots while attaining the target speed. Whereas, significant overshoots and undershoots are seen with PWM control (figure 5). Small such oscillations are also seen with FOC control. Torque Ripple quantifies unwanted torque fluctuations causing vibration (lower % is better), where the FOC (10%) offers the best performance and PWM Control (100%) shows highest torque ripples.

3. Conclusion

This paper presents dynamic response analysis of different speed control techniques particularly focusing on torque ripple contents. While simple and cost-effective, conventional PWM methods inherently produce significant commutation torque ripple and harmonic distortion due to trapezoidal back-EMF and phase current discontinuities. Its performance is generally inadequate for demanding EV drive comfort and efficiency requirements. SMC demonstrates strong robustness against parameter variations and load disturbances. It effectively reduces torque ripple compared to basic PWM with hardly any overshoot or undershoot. The FOC control appears to be most effective technique for minimizing torque

ripple. By decoupling torque and flux production and enabling smooth sinusoidal current control, FOC fundamentally addresses the source of commutation ripple inherent in BLDC motors. Its steady-state error falls within 1% and torque ripple of just 10% leads to smoother operation of the BLDC motor.

References

[1] D. Mohanraj *et al*., "A Review of BLDC Motor: State of Art, Advanced Control Techniques, and Applications," in *IEEE Access*, vol. 10, pp. 54833-54869, 2022, doi: 10.1109/ACCESS.2022.3175011

[2] K. A. Gore and R. T. Ugale, "Design and Comparative Analysis of PMSM, BLDC, SynRM, and PMAssi-SynRM Motors for Two-Wheeler Electric Vehicle Application," *2022 IEEE Conference on Interdisciplinary Approaches in Technology and Management for Social Innovation (IATMSI)*, Gwalior, India, 2022, pp. 1-6, doi: 10.1109/IATMSI56455.2022.10119363.

[3] Z. Wang, T. W. Ching, S. Huang, H. Wang and T. Xu, "Challenges Faced by Electric Vehicle Motors and Their Solutions," in *IEEE Access*, vol. 9, pp. 5228-5249, 2021, doi: 10.1109/ACCESS.2020.3045716

[4] N. Soni and M. Barai, "Performance Study of Regenerative Braking of BLDC Motor targeting Electric Vehicle Applications," *2022 2nd Asian Conference on Innovation in Technology (ASIANCON)*, Ravet, India, 2022, pp. 1-6, doi: 10.1109/ASIANCON55314.2022.9909322.

[5] R. M. Pindoriya, B. S. Rajpurohit, R. Kumar and K. N. Srivastava, "Comparative analysis of permanent magnet motors and switched reluctance motors capabilities for electric and hybrid electric vehicles," *2018 IEEMA Engineer Infinite Conference (eTechNxT)*, New Delhi, India, 2018, pp. 1-5, doi: 10.1109/ETECHNXT.2018.8385282.

[6] M. Monadi, M. Nabipour, F. Akbari-Behbahani and E. Pouresmaeil, "Speed Control Techniques for Permanent Magnet Synchronous Motors in Electric Vehicle Applications Toward Sustainable Energy Mobility: A Review," in *IEEE Access*, vol. 12, pp. 119615-119632, 2024, doi: 10.1109/ACCESS.2024.3450199.

[7] C. R. Edwin Selva Rex, K. Neelima, P. Bhavana, Y. Gayathri, K. Bhargava and S. V. Kumar, "Speed Control of BLDC Motor Using Trapezoidal Commutation & PWM

Technique," *2023 4th IEEE Global Conference for Advancement in Technology (GCAT)*, Bangalore, India, 2023, pp. 1-5, doi: 10.1109/GCAT59970.2023.10353285.

[8] K. S, K. Nanshikar, S. Das and S. A, "Analysis of Control Methods for BLDC Motors in Electric Vehicle Powertrain Systems," *2024 IEEE International Conference on Power Electronics, Drives and Energy Systems (PEDES)*, Mangalore, India, 2024, pp. 1-6, doi: 10.1109/PEDES61459.2024.10961105.

[9] G. Gupta and M. Sreejeth, "Comparative analysis of Speed control of BLDC motor using PWM and Current Control Techniques," *2022 IEEE IAS Global Conference on Emerging Technologies (GlobConET)*, Arad, Romania, 2022, pp. 610-614, doi: 10.1109/GlobConET53749.2022.9872173.

[10] J. Lee, G. C. Lim and J. -I. Ha, "Pulse Width Modulation Methods for Minimizing Commutation Torque Ripples in Low Inductance Brushless DC Motor Drives," in *IEEE Transactions on Industrial Electronics*, vol. 70, no. 5, pp. 4537-4547, May 2023, doi: 10.1109/TIE.2022.3189104.

[11] R. L. Valle, P. M. De Almeida, G. A. Fogli, A. A. Ferreira and P. G. Barbosa, "Simple and Effective Digital Control of a Variable-Speed Low Inductance BLDC Motor Drive," in *IEEE Access*, vol. 8, pp. 13240-13250, 2020, doi: 10.1109/ACCESS.2020.2966437

[12] C. -L. Huang, F. -C. Lee, C. -J. Liu, J. -Y. Chen, Y. -J. Lin and S. -C. Yang, "Torque Ripple Reduction for BLDC Permanent Magnet Motor Drive Using DC-Link Voltage and Current Modulation," in *IEEE Access*, vol. 10, pp. 51272-51284, 2022, doi: 10.1109/ACCESS.2022.3173325.

[13] P. Shah, P. Ubare, D. Ingole and D. Sonawane, "Performance Improvement of BLDC Motor Speed Control Using Sliding Mode Control and Observer," *2021 International Symposium of Asian Control Association on Intelligent Robotics and Industrial Automation (IRIA)*, Goa, India, 2021, pp. 247-252, doi: 10.1109/IRIA53009.2021.9588766.

[14] K. Guo, M. Yang, X. Li, P. Shi and P. Wang, "Research on a New Adaptive Integral Sliding Mode Controller Based on a Small BLDC," in *IEEE Access*, vol. 10, pp. 73204-73213, 2022, doi: 10.1109/ACCESS.2022.3188665.

[15] N. Prabhu, R. Thirumalaivasan and B. Ashok, "Critical Review on Torque Ripple Sources and Mitigation Control Strategies of BLDC Motors in Electric Vehicle Applications," in *IEEE Access*, vol. 11, pp. 115699-115739, 2023, doi: 10.1109/ACCESS.2023.3324419

[16] S. S. Rauth and B. Samanta, "Comparative Analysis of IM/BLDC/PMSM Drives for Electric Vehicle Traction Applications Using ANN-Based FOC," *2020 IEEE 17th India Council International Conference (INDICON)*, New Delhi, India, 2020, pp. 1-8, doi: 10.1109/INDICON49873.2020.9342237.

[17] M. Kumar, S. Tiwari, V. Kumar, S. J. Sampathi and R. Kumar Jarial, "Implementation of Field-Oriented Control (FOC) Algorithm for Brushless DC (BLDC) Motor Speed Regulation," *2023 Second IEEE International Conference on Measurement, Instrumentation, Control and Automation (ICMICA)*, Kurukshetra, India, 2024, pp. 1-6, doi: 10.1109/ICMICA61068.2024.10732537.

[18] R. Jauhar, N. Ismail and N. Sartika, "Design of Torque Controller Based on Field Oriented Control (FOC) Method on BLDC Motor," *2022 16th International Conference on Telecommunication Systems, Services, and Applications (TSSA)*, Lombok, Indonesia, 2022, pp. 1-5, doi: 10.1109/TSSA56819.2022.10063889.

[19] K. Kolano, "Improved Sensor Control Method for BLDC Motors," in *IEEE Access*, vol. 7, pp. 186158-186166, 2019, doi: 10.1109/ACCESS.2019.2960580.

[20] M. S. Patil, R. Medhane and S. S. Dhamal, "Comparative Analysis of Various DTC Control Techniques on BLDC Motor for Electric Vehicle," *2020 7th International Conference on Smart Structures and Systems (ICSSS)*, Chennai, India, 2020, pp. 1-6, doi: 10.1109/ICSSS49621.2020.9201982.

[21] N. Prabhu, R. Thirumalaivasan and B. Ashok, "Critical Review on Torque Ripple Sources and Mitigation Control Strategies of BLDC Motors in Electric Vehicle Applications," in *IEEE Access*, vol. 11, pp. 115699-115739, 2023, doi: 10.1109/ACCESS.2023.3324419.

[22] D. Mohanraj, J. Gopalakrishnan, B. Chokkalingam and L. Mihet-Popa, "Critical Aspects of Electric Motor Drive Controllers and Mitigation of Torque Ripple—Review," in *IEEE Access*, vol. 10, pp. 73635-73674, 2022, doi: 10.1109/ACCESS.2022.3187515

[23] A. R. S and B. L. S, "Techniques for Torque Ripple Reduction in BLDC Motor for EV," *2023 International Conference on Circuit Power and Computing Technologies (ICCPCT)*, Kollam, India, 2023, pp. 1008-1014, doi: 10.1109/ICCPCT58313.2023.10245720